Diffusion-weighted MR imaging of the breast: comparison of apparent diffusion coefficient values of normal breast tissue with benign and malignant breast lesions

Sebnem Orguc[1], MD, *Isil Basara*[1], MD, *Teoman Coskun*[2], MD

INTRODUCTION The specificity of conventional magnetic resonance (MR) imaging is lower than its high sensitivity. Diffusion-weighted imaging (DWI), based on alterations in the microscopic motion of water molecules, promises improved specificity for breast MR imaging. In this study, we aimed to determine the diagnostic potential of DWI to differentiate between benign and malignant breast lesions and normal breast tissue.

METHODS Dynamic contrast-enhanced breast MR imaging and DWI were applied to 108 women. Apparent diffusion coefficient (ADC) values were obtained for normal breast tissue (n = 183), benign lesions (n = 66) and malignant lesions (n = 58). The results were compared with the patients' final diagnoses.

RESULTS Mean ADC values for benign and malignant breast lesions were $1.04 \times 10^{-3} \pm 0.29 \times 10^{-3}$ mm^2/s and $2.00 \times 10^{-3} \pm 0.55 \times 10^{-3}$ mm^2/s, respectively (p = 0.001, Student's *t*-test), while that for normal breast tissue was $1.78 \times 10^{-3} \pm 0.33 \times 10^{-3}$ mm^2/s. With a cut-off value of 1.46×10^{-3} mm^2/s for ADC in receiver operating characteristic analysis, 95% sensitivity and 85% specificity were achieved for differentiating between benign and malignant lesions.

CONCLUSION DWI of the breast can help differentiate benign and malignant breast lesions from normal breast tissue. DWI, which can be easily introduced into standard breast MR imaging protocols without increasing imaging times, promises to increase the accuracy of breast MR imaging without contrast media. However, its clinical value will depend on the standardisation of b-values and other technical parameters in larger future study series.

Keywords: apparent diffusion coefficient, breast cancer, breast tumour, diffusion-weighted imaging, magnetic resonance imaging
Singapore Med J 2012; 53(11): 737–743

INTRODUCTION

Dynamic contrast-enhanced magnetic resonance imaging (DCE-MRI) is increasingly used as a problem-solving tool to identify and characterise breast lesions in selected patients.[1,2] The sensitivity of magnetic resonance (MR) imaging is reported to be as high as 89%–100%.[3,4] However, overlaps between findings for benign and malignant lesions on conventional breast MR imaging have led to variable specificities for breast lesions.[5-7] Since the specificity of conventional MR imaging, which uses morphological and kinetic criteria, is relatively lower than its high sensitivity, advanced MR imaging application has a potential role to play in the diagnosis of breast lesions. Diffusion-weighted imaging (DWI) promises improved specificity of breast MR imaging.[8-10] In this prospective study, we aimed to determine the diagnostic potential of DWI for differentiating between benign and malignant lesions of the breast and normal breast tissue.

METHODS

We applied DCE-MRI and DWI using a 1.5 Tesla MR system (Signa HDx; General Electric, Madison, WI, USA) and bilateral 8-channel high-density breast coil to 108 consecutive women. The patients were prospectively enrolled in our study with various indications for conventional breast MR imaging between November 2009 and July 2011, with no specific exclusion criteria. The study was approved by the local ethics committee, and all the patients provided written informed consent.

The standard sequences for conventional breast MR imaging included axial short tau inversion recovery (STIR), sagittal fast spin-echo fat-saturated T2-weighted and sagittal 3D Vibrant (post-contrast dynamic fat-saturated T1-weighted sequence optimised for breast imaging) sequences. DWI with b-values of 0 s/mm^2 and 600 s/mm^2 were applied in the axial plane prior to the application of contrast material. The other parameters for DWI were: (a) sequence (echo-planar imaging); (b) repetition time (TR)/time to echo (TE): 7,900 ms/88.9 ms (minimum TE); (c) field of view: 36–40 mm; (d) matrix: 192 × 192; (e) slice thickness/interval: 5 mm/1 mm; (f) NEX (square root of the number of acquisitions): 16; (g) rBW (receive bandwidth): 250 kHz; and (h) imaging time: 261 s.

After acquisition, all data were transferred to a workstation (Advantage Windows 4.4; General Electric, Madison, WI, USA). During post-processing, black-and-white apparent diffusion

[1]Department of Radiology, [2]Department of General Surgery, Celal Bayar University of Medicine, Manisa, Turkey
Correspondence: Dr Isil Basara, 194 sok, 46/12 Gencalp Apt, 35040 Bornova, Izmir, Turkey. slbasara@hotmail.com

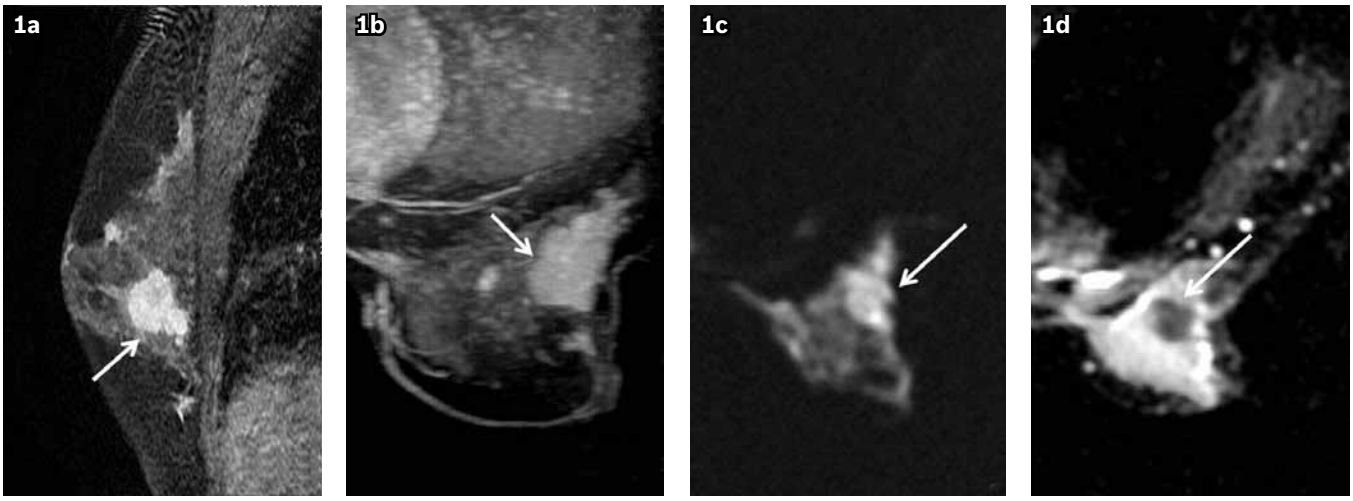

Fig. 1 Histopathological findings in a 43-year-old woman with invasive ductal carcinoma. (a) Postcontrast T1-W fat-saturated sagittal image and (b) MIP image of the breast in the axial plane show an enhancing BI-RADS 5 lesion with irregular margins (arrows). (c) DWI with b = 600 and (d) ADC map show a mass with restricted diffusion that was hyperintense on DWI and hypointense on ADC map (arrows). Mean ADC value = 0.95 × 10^{-3} mm^2/s.
ADC: apparent diffusion coefficient; BI-RADS: Breast Imaging Reporting and Data System; DWI: diffusion-weighted imaging; MIP: maximum intensity projection

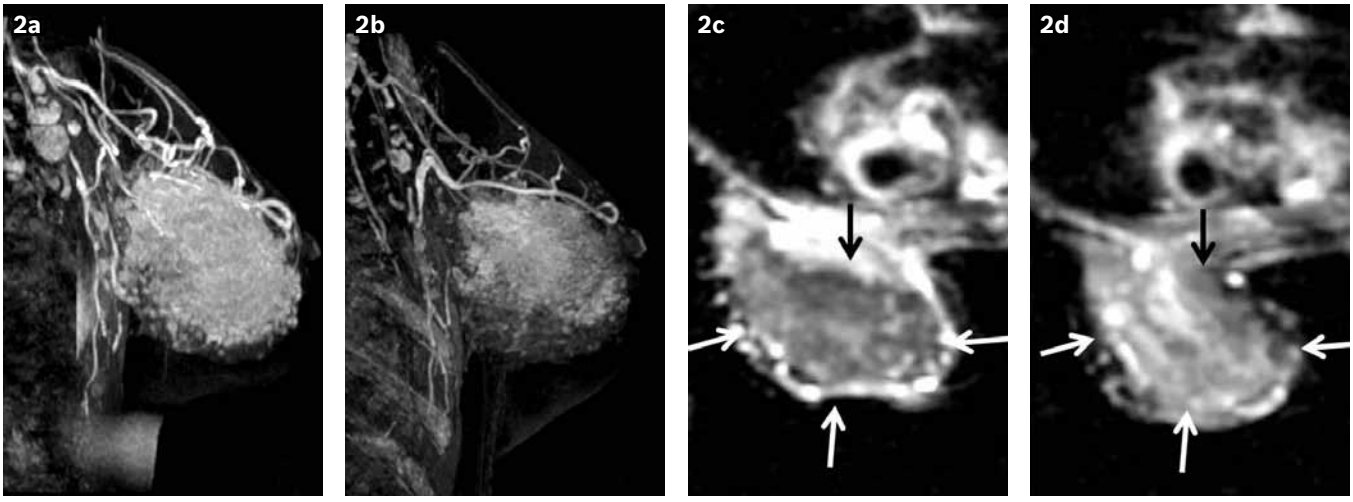

Fig. 2 Histopathological findings in a 43-year-old woman with locally advanced invasive ductal carcinoma. Sagittal MIP reconstructions obtained from the first series of post-contrast dynamic images (a) before and (b) after neoadjuvant chemotherapy show minimal decrease in the size of tumour, axillary lymph nodes and vascularity. ADC maps of DWI (c) before (b = 0) and (d) after (b = 600) neoadjuvant chemotherapy are also seen (black and white arrows show the margin of the lesion). Mean ADC value: before, 0.93 × 10^{-3} mm^2/s; after, 1.08 × 10^{-3} mm^2/s. Post-therapy measurements were not included in the study.
ADC: apparent diffusion coefficient; DWI: diffusion-weighted imaging; MIP: maximum intensity projection

coefficient (ADC) maps were generated, and the ADC values of normal breast tissue for each patient and the lesions that could be visualised were measured. The ADC values of breast tissue were obtained from the fibroglandular areas while trying to omit the fatty tissue in the region of interest (ROI). For breasts with a dominant fatty pattern, a small ROI was used to minimise the inclusion of fat, as fat may artificially lower ADC values. For lesions, the ROI was placed over the tumour while trying to avoid areas of haemorrhage or necrosis. ADC measurement inevitably included debris and the liquefied part of infiltrative inflammatory lesions and abscesses, as wall thickness was insufficient for the placement of ROI. The sizes of ROI were 10–100 mm^2.

The mean age of the patients was 44.9 (range 19–77) years. There was no difference between the mean age of patients with malignant and benign lesions (45.0 years vs. 44.8 years, p = 0.9; Student's *t*-test). The ADC measurements of normal breast tissue were obtained from 183 breasts. Unilateral mastectomy, post-radiation changes, postoperative changes and diffuse involvement of disease obscured normal breast tissue measurement in 33 patients. The ADC values of 134 breast lesions were obtained from a total of 93 patients.

On histopathological examination, 58 lesions proved to be malignant in 42 patients: invasive ductal carcinoma (IDC) n = 31 (Figs. 1 & 2); invasive lobular carcinoma (ILC) n = 1; mixed invasive lobular and ductal carcinoma (IDC+ILC) n = 3; ductal carcinoma in situ n = 2; mix IDC + mucinous carcinoma n = 1; IDC and pleomorphic carcinoma n = 1; medullary carcinoma n = 1; malignant phyllodes tumour n = 1; diffuse leukaemic infiltration of the breast n = 1 (Fig. 3). The mean size of the malignant lesions was 41.3 ± 34.3 mm.

A total of 66 benign lesions in 44 patients were included in the study. 35 lesions were histopathologically diagnosed as benign

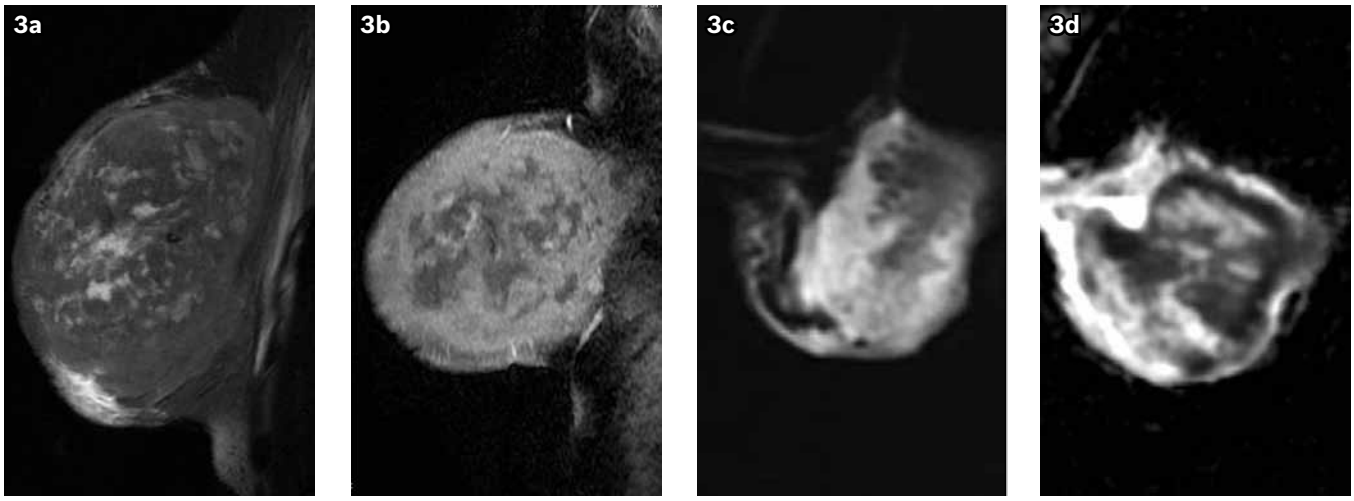

Fig. 3 Histopathological findings in a 32-year-old woman showing leukaemic infiltration of the breast. (a) T2-W sagittal and (b) post-contrast T1-W fat-saturated subtracted sagittal images show a huge lesion with central areas of necrosis. (c) DWI with b = 600 and (d) ADC map show solid portions of the mass with restricted diffusion that were hyperintense on DWI and hypointense on ADC map. Mean ADC value = 0.31 × 10^{-3} mm^2/s. The necrotic central part of the tumour, with relatively higher diffusion, was not included in the ROI during measurements.
ADC: apparent diffusion coefficient; DWI: diffusion-weighted imaging; ROI: region of interest

fibroadenoma (n = 18) (Fig. 4), cystosarcoma phyllodes tumour (n = 2), fibrocystic changes (n = 4), seroma (n = 6), fat necrosis (n = 2), ductal hyperplasia (n = 1), papilloma (n = 1) and haematoma (n = 1). 31 benign lesions had typical BI-RADS (Breast Imaging Reporting and Data System) 2 findings on DCE-MRI and were diagnosed as cyst (n = 7), fibroadenoma (n = 20) and intramammarian lymph node (n = 4) (Fig. 5). There were 11 fibroadenomas that showed no increase in dimensions for at least two years compared to previous breast imaging studies. The follow-up periods of the remaining 20 lesions were less than two years. However, these were included in the study, as they showed definite benign imaging characteristics that were categorised as BI-RADS 2. The mean size of the benign lesions was 16.7 ± 11.3 mm, which was significantly smaller than that of the malignant ones (p = 0.001, Student's *t*-test). The ADC values of ten lesions in seven patients with infectious disease of the breast were measured. The diagnoses of these patients were confirmed as granulomatous mastitis (n = 5), infected galactocele (n = 1) and tuberculosis abscess (n = 1) (Fig. 6).

Three patients with locally advanced breast carcinoma, one patient with leukaemic infiltration and three patients with granulomatous mastitis were diagnosed on core biopsy. Seven patients with seroma, one patient with infected galactocele, one patient with tuberculosis abscess and one patient with a haematoma were diagnosed by needle aspiration biopsy. The histopathological results of all other malignant and benign lesions were confirmed by surgical excision.

RESULTS

All malignant lesions, except an IDC measuring 4 mm in diameter, could be visualised on the ADC maps. Benign lesions < 1 cm in diameter with ADC values similar to breast tissue were more difficult to detect. For such patients, the coordinates of the lesion were correlated with post-contrast images. DWI images were

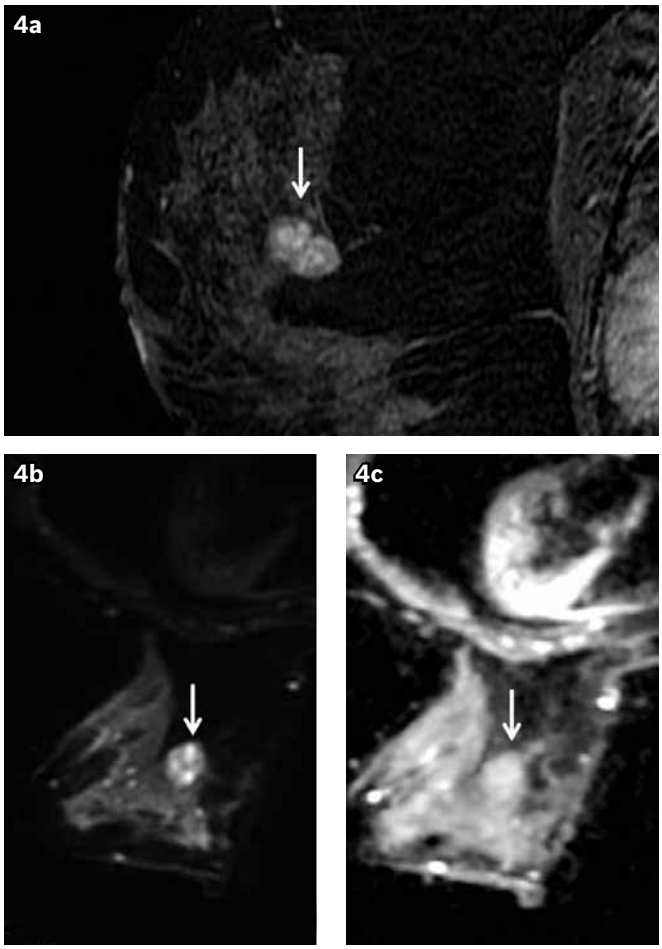

Fig. 4 Histopathological findings in a 39-year-old woman with fibroadenoma. (a) Post-contrast T1-W fat-saturated subtracted sagittal image shows a BI-RADS 2 solid mass typical of a fibroadenoma with macrolobulated contour, smooth margins, dark internal septa and type I enhancement characteristics (arrow). (b) DWI with b = 600 and (c) ADC map show a fibroadenoma (arrows) that exhibited no restriction of diffusion. Mean ADC value of 2.17 × 10^{-3} mm^2/s was higher than that of neighbouring glandular tissue (1.97 × 10^{-3} mm^2/s).
ADC: apparent diffusion coefficient; BI-RADS: Breast Imaging Reporting and Data System; DWI: diffusion-weighted imaging

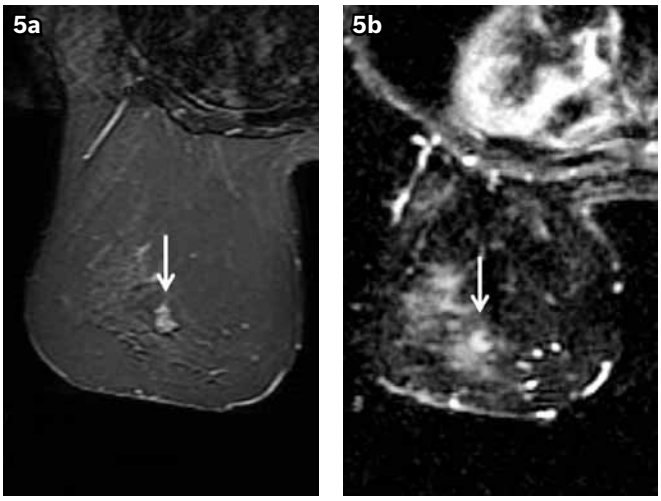

Fig. 5 Histopathological findings in a 61-year-old woman with intramammarian lymph node. (a) Axial STIR image shows an intramammarian lymph node (arrow), with a typical hilar notch, that was stable on screening mammograms. (b) ADC map shows a mean ADC value = 2.14 × 10^{-3} mm^2/s of the lymph node (arrow).
ADC: apparent diffusion coefficient; STIR: short tau inversion recovery

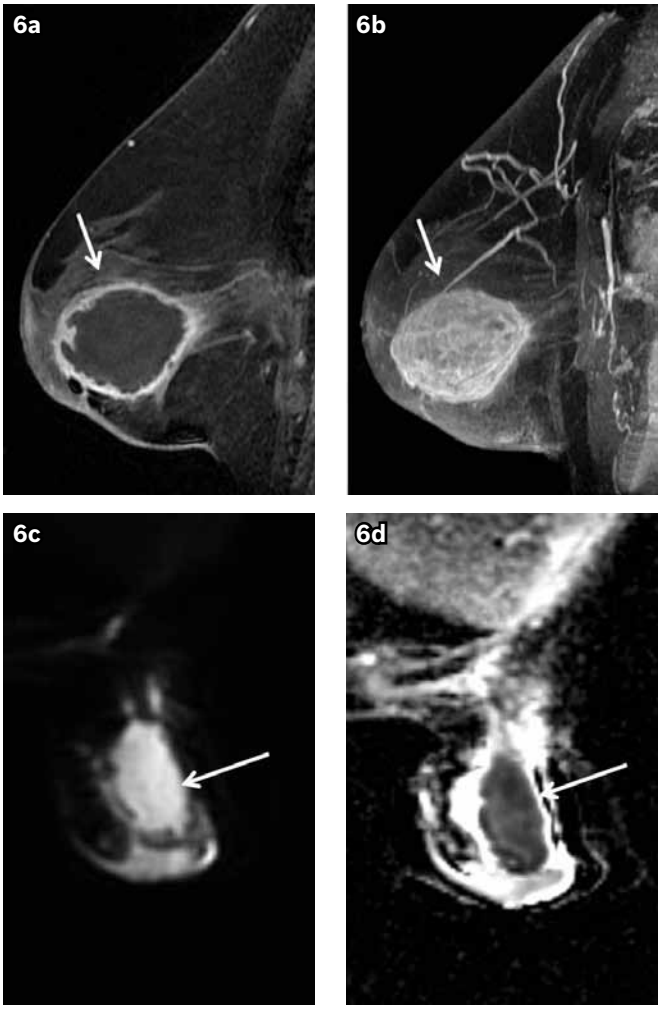

Fig. 6 Histopathological findings in a 67-year-old woman with tuberculosis abscess. (a) Post-contrast T1-W fat-saturated sagittal image (arrow) and (b) MIP image of the breast in the sagittal plane show a mass lesion with enhancing thick irregular wall (arrow). (c) DWI with b = 600 shows a lesion with high signal (arrow). (d) ADC map shows marked restriction of diffusion in the central part of the abscess (arrow). Mean ADC value = 0.57 × 10^{-3} mm^2/s.
ADC = apparent diffusion coefficient; DWI = diffusion-weighted imaging; MIP = maximum intensity projection

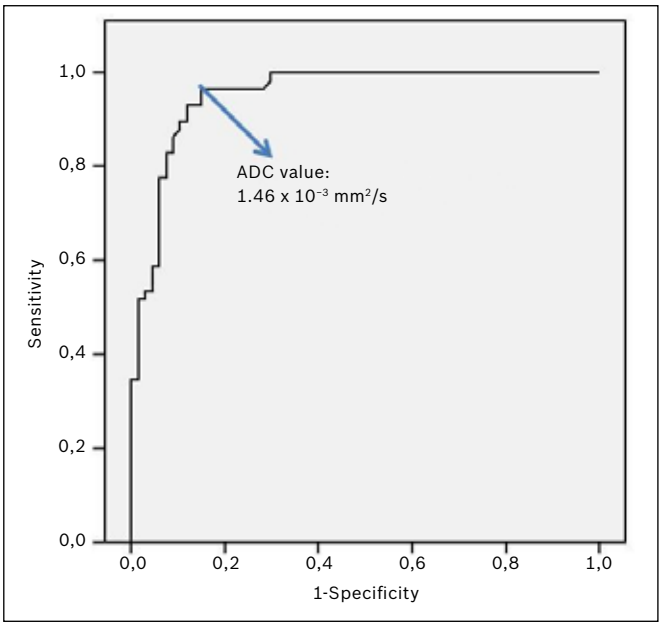

Fig. 7 ROC analysis of the ADC values of 124 breast lesions (malignant, n = 58; benign, n = 66). The ADC value of 1.46 × 10^{-3} mm^2/s as cut-off score provided 95% sensitivity and 85% specificity for the classification of benign and malignant lesions. Area under the curve = 0.95; standard error = 0.017; asymptotic 95% confidence interval = 0.919–0.988; asymptotic significance (b) = 0.000.
ADC: apparent diffusion coefficient; ROC: receiver operating characteristic

non-diagnostic in three patients secondary to motion artefacts and were excluded from the study. No focal lesions were found in seven patients. When the ADC values of 124 breast lesions (malignant n = 58; benign n = 66) and 183 normal breast tissues were evaluated, the mean ADC value was 2.00 × 10^{-3} ± 0.55 × 10^{-3} mm^2/s for benign lesions and 1.04 × 10^{-3} ± 0.29 × 10^{-3} mm^2/s for malignant ones. The difference between the ADC values of benign and malignant lesions was statistically significant (p = 0.001; Student's *t*-test). The cut-off value was determined by the peak of the receiver operating characteristic (ROC) curve, which yielded optimal sensitivity and specificity, so that the numbers of false negative and false positive cases were in an acceptable range. When a cut-off value of 1.46 × 10^{-3} mm^2/s was selected as the ADC value in the ROC analysis, it achieved 95% sensitivity and 85% specificity for differentiating between benign and malignant breast lesions (Fig. 7). The mean ADC value of infectious lesions of the breast was determined as 1.05 × 10^{-3} mm^2/s (range 0.57 × 10^{-3} to 2.61 × 10^{-3} mm^2/s). The mean ADC value of the 183 normal breast tissues was calculated as 1.78 × 10^{-3} ± 0.33 × 10^{-3} mm^2/s, which differed significantly from that of the malignant lesions.

DISCUSSION

Breast MR imaging is increasingly used for the detection, diagnosis and staging of breast cancer.[1,2] During breast MR imaging, T1-weighted, T2-weighted and dynamic post-contrast series are used, and a combination of morphological and kinetic features are applied to obtain high sensitivity. However, hormonal and proliferative changes, fibroadenomas and papillomas that

Table I. Review of the literature on findings of diffusion-weighted imaging and apparent diffusion coefficient values.

Study	Malignant lesion		Benign lesion		b-value	Normal tissue	
	DWI* ($\times 10^{-3}$ mm^2/s)	ADC† (cm)	DWI* ($\times 10^{-3}$ mm^2/s)	ADC† (cm)		DWI* ($\times 10^{-3}$ mm^2/s)	ADC† (cm)
Marini et al[6]	0.95 ± 0.18	2.21	1.48 ± 0.37	1.92	0–1,000	NA	NA
Guo et al[9]	0.97 ± 0.20	2.75 (0.4–6)	1.57 ± 0.23	2.64 (0.5–9)	0–1,000	NA	NA
Kinoshita et al[14]	1.22 ± 0.19	2.7 (0.8–8)	1.495 ± 0.181	1.7 (1–3)	0–700	NA	NA
Woodhams et al[16]	1.12 ± 0.24	2.2 (0,7–7)	1.51 ± 0.068	NA	0–750–1,000	2.05 ± 0.27	NA
Woodhams et al[24]	1.22 ± 0.31	3.68 (0.7–6)	1.67 ± 0.54	3.4 (0.5–11)		2.09 ± 0.27	NA
Ruboseva et al[25]	0.95 ± 0.027	NA	NA	NA	0–200–400–600–1,000	NA	NA
Kuroki et al[26]	1.12 ± 0.23	2.43	1.448 ± 0.45	NA	0–1,000	NA	NA
Hatakenaka et al[27]	1.15 ± 0.26	2.65 ± 1.28	1.66 ± 0.30	2.14 ± 0.76	0–500–1,000	NA	NA
Luo et al[28]	0.87 ± 0.23	3.2 (1.6–5.1)	1.59 ± 0.26	1.6 (0.5–2.1)	0–500–1,000	1.98 ± 0.31	NA
Pereira et al[30]	0.92 ± 0.26	3.09 (1.0–11.2)	1.50 ± 0.34	1.68 (0.8–4.7)	0–250–500–750–1,000	NA	NA
Sinha and Sinha[32]	1.01 ± 0.17	NA	NA	NA	0–500–1,000–1,500–1,800	1.63 ± 0.22	NA
Present study	1.04 ± 0.29	4.13 ± 3.43	2.00 ± 0.55	1.67 ± 1.13	0–600	1.78 ± 0.33	NA

*Values expressed as mean ± SD. † Values expressed as mean (range) or mean ± SD.

ADC: apparent diffusion coefficient; DWI: diffusion-weighted imaging; NA: not available; SD: standard deviation

give rise to false positive results lower the specificity of breast MR imaging considerably.

DWI is an advanced MR imaging technique based on the diffusion signal of tissues, which reflects the amount of random motion of water molecules into tissues due to thermal agitation (Brownian motion).[9,11,12] DWI was first introduced for acute cerebral infarction, for which it has become one of the primary imaging modalities. However, it is now being used for other clinical applications over the entire body, and holds great promise for the detection and characterisation of tumours of other organs such as the ovaries, pancreas, prostate and breast.[9,12-19] DWI helps in the investigation of breast masses by providing information about the biological behaviour of the tumour.[11] Several studies have evaluated breast lesions using DWI.[9,12,14,16]

DWI has been reported to be a useful technique for the discrimination of benign and malignant lesions.[9,12,14,16,20] Malignant lesions with tightly packed cells have a reduced extracellular space, resulting in decreased diffusion of water. The result is a high DWI signal intensity and a lower ADC value, indicating restricted diffusion on an ADC map (Figs. 1–3). On the contrary, benign lesions with a larger extracellular space have water molecules that are more mobile, and thus higher ADC values (Figs. 4 & 5).[21-23] Similar to the findings of other reports in the literature, our finding, which was based on the ADC values of 58 malignant lesions, 66 benign lesions and 183 normal breast tissues, supports the consensus that DWI can successfully differentiate between benign and malignant lesions (Table I).[6,9,14,16,23-28,30,32]

In a meta-analysis of 12 studies, Tsushima et al reported that the ADC values of benign breast tumours were between 1.41 × 10^{-3} mm^2/s and 2.01 × 10^{-3} mm^2/s, and those of malignant lesions were in the range of 0.90 × 10^{-3} mm^2/s to 1.61 × 10^{-3} mm^2/s.[22] The mean ADC values of normal breast tissue in our study were in the range of 1.51 × 10^{-3} mm^2/s to 2.37 × 10^{-3} mm^2/s. The mean ADC value for malignant lesions was found to be 1.04 × 10^{-3} ± 0.29 × 10^{-3} mm^2/s, which was compatible with that reported in the literature.

The cut-off ADC value in our series was determined on the basis of the maximum ADC value that gave a specificity of 95% in the ROC analysis. The specificity and sensitivity of reports in the literature based on the cut-off values selected are summarised in Table II.[6,9,16,25,27,28,30] The findings of statistical analysis in our series were similar to those in the literature. The mean ADC of benign lesions in our study also showed a value within the reported range, although it was at the higher end. It is possible that the inclusion of patients with fibrocystic changes and seromas in the study population may have increased the mean ADC value slightly.

When the range of ADC values was considered, a slight overlap was observed in the ADC values of benign and malignant lesions, both in the literature and in our series. Some benign conditions, such as haematomas, abscesses, fibrosis and inflammatory lesions, are known to exhibit low ADC values.[31] Due to the wide range of ADC values reported in patients with inflammatory diseases and the false positive results known in this group of patients, these patients were not included in the benign group for statistical analysis in our study. Mucinous carcinomas with high mucine content have also been reported to contribute to high ADC values.[27] On the contrary, the mucinous and medullary carcinomas in our series exhibited low ADC values. As ADC values have been reported to be higher in the central necrotic

Table II. Review of the literature on the discrimination between benign and malignant lesions based on diffusion-weighted imaging and cut-off apparent diffusion coefficient values.

Study	Cut-off ADC values ($\times 10^{-3}$ mm^2/s)	Sensitivity (%)	Specificity (%)
Marini et al[6]	1.1	80	81
Guo et al[9]	1.30	93	88
Woodhams et al[16]	1.60	93	46
Ruboseva et al[25]	1.13	86	86
Hatakenaka et al[27]	1.48	83.9	81.3
Luo et al[28]	1.22	88.9	87.9
Pereira et al[30]	1.21	92.3	92.3
Present study	1.46	95	85

ADC: apparent diffusion coefficient

areas of malignant tumours,[29,30] they were measured from the periphery of necrotic tumours in our series.

DWI provides qualitative and quantitative information related to tumour cellularity as ADC is a quantitative measurement reflecting the free motion of water molecules, which is inversely proportional to the tumour cellular density.[20] High cellularity, intracellular and extracellular oedema, high viscosity and high grade of fibrosis decrease the mobility of water molecules, resulting in restricted diffusion in DWI.[16,23,24] The microscopic movement of biological tissues consist of molecular diffusion in the extracellular compartment and microcirculation of blood in the capillary network (flow). Therefore, perfusion is another factor that affects ADC values. ADC values also differ with various b-values, as seen in the literature. Images with low b-values result in less diffusion-weighted images, as a lower gradient is applied. Also, the extension of microvascular structures in malignant lesions may increase the perfusion effect on ADC values in images with low b-values.[11,14,16] However, the signal-to-noise ratio in these images is higher than that in diffusion images with high b-values.

The variations seen in the ADC values of previous reports can be explained by the difference in their b-values (0–1,074 s/mm^2), other technical factors and variations in the pathologies included in these series. Typically, at least two b-values should be used during DWI in order to enable meaningful ADC interpretation, although accuracy increases when more b-values are used. Woodhams et al reported that b < 750 mm^2/s was highly efficient in detecting breast masses.[16] Pereira et al, however, reported no significant difference between the ADC values of benign and malignant lesions when different combinations of b-values were used, and thus concluded that using multiple b-values in a DWI sequence was unnecessary.[30] In our study, we had used b-values of 0 s/mm^2 and 600 s/mm^2 in order to limit the examination time.

The diagnostic accuracy of DWI for breast can only be ascertained once technical parameters and post-processing procedures are standardised for the modality. Major technical limitations associated with it are distortion of the images secondary to susceptibility, chemical shift, motion artefacts and low spatial resolution. Even under optimal circumstances, small lesions may not be visualised on ADC maps, as Kinoshita et al have reported that lesions < 10 mm in diameter cannot be demonstrated by DWI.[14] Another limitation is that of non-mass-like enhancing lesions that form large and non-compact lesions with normal parenchyma intervening within the tumour. Non-IDCs, lobular carcinoma in situ, atypical ductal hyperplasia, papillomas, hormonal changes and fibrocystic disease may show this type of enhancement.[33] According to Guo et al[9] and Sinha et al,[12] the mean ADC value is inversely proportional to cellular density, and therefore, these lesions may exhibit less restriction of diffusion. Finally, it should be noted that DWI cannot replace dynamic breast MR imaging with contrast, but can be used as a complementary technique to evaluate breast masses. DWI may also provide a useful alternative in cases where contrast media is contraindicated for patients.[16,34,35]

To summarise, DWI is a valuable tool that can be used to analyse the molecular characteristics of tissue *in vivo*. It visualises and quantifies the random motions of molecules and provides additional diagnostic information for the differential diagnosis of enhancing breast lesions. Short acquisition times and no need for contrast material make it an easy adjunct to standard breast MR imaging protocol. With an ADC cut-off value of 1.46×10^{-3} mm^2/s in the ROC analysis, we were able to achieve a sensitivity of 95% and specificity of 85% when differentiating between benign and malignant lesions in our study population using DWI. The ADC values obtained from our study were compatible with those in the literature. Our results support the consensus that DWI of the breast has the diagnostic potential to differentiate benign and malignant lesions of the breast from normal breast tissue.

REFERENCES

1. Orel SG, Schnall MD. MR imaging of the breast for the detection, diagnosis, and staging of breast cancer. Radiology 2001; 220:13-30.
2. Ikeda DM, Baker DR, Daniel BL. Magnetic resonance imaging of breast cancer : clinical indications and breast MRI reporting system. J Magn Reson Imaging 2000; 12:975-83.
3. Kuhl C. The current status of breast MR imaging. Part I. Choice of technique, image interpretation, diagnostic accuracy, and transfer to clinical practice. Radiology 2007; 244:356-78.
4. Bedrosian I, Mick R, Orel SG, et al. Changes in the surgical management of patients with breast carcinoma based on preoperative magnetic resonance

imaging. Cancer 2003; 98:468-73.
5. Macura KJ, Ouwerkerk R, Jacobs MA, Bluemke DA. Patterns of enhancement on breast MR images: interpretation and imaging pitfalls. Radiographics 2006; 26:1719-34.
6. Marini C, Iacconi C, Giannelli M, et al. Quantitative diffusion-weighted MR imaging in the differential diagnosis of breast lesion. Eur Radiol 2007; 17:2646-55.
7. Fischer U, Kopka L, Grabbe E. Breast carcinoma: effect of preoperative contrast-enhanced MR imaging on the therapeutic approach. Radiology 1999; 213:881-8.
8. Wenkel E, Geppert C, Schulz-Wendtland R, et al. Diffusion weighted imaging in breast MRI: comparison of two different pulse sequences. Acad Radiol 2007; 14:1077-83.
9. Guo Y, Cai YQ, Cai ZL, et al. Differentiation of clinically benign and malignant breast lesions using diffusion-weighted imaging. J Magn Reson Imaging 2002; 16:172-8.
10. Partridge SC, De Martini WB, Kurland BF, et al. Quantitative diffusion-weighted imaging as an adjunct to conventional breast MRI for improved positive predictive value. AJR Am J Roentgenol 2009; 193:1716-22.
11. Bammer R. Basic principles of diffusion-weighted imaging. Eur J Radiol 2003; 45:169-84.
12. Sinha S, Lucas-Quesada FA, Sinha U, DeBruhl N, Bassett LW. In vivo diffusion-weighted MRI of the breast: potential for lesion characterization. J Magn Reson Imaging 2002; 15:693-704.
13. Hosseinzadeh K, Schwarz SD. Endorectal diffusion-weighted imaging in prostate cancer to differentiate malignant and benign peripheral zone tissue. J Magn Reson Imaging 2004; 20:654-61.
14. Kinoshita T, Yashiro N, Ihara N, et al. Diffusion-weighted half-Fourier single-shot turbo spin echo imaging in breast tumor: differentiation of invasive ductal carcinoma from fibroadenoma. J Comput Assist Tomogr 2002; 26:1042-6.
15. Ichikawa T, Haradome H, Hachiya J, Nitatori T, Araki T. Diffusion-weighted MR imaging with a single-shot echoplanar sequence: detection and characterization of focal hepatic lesions. AJR Am J Roentgenol 1998; 170:397-402.
16. Woodhams R, Matsunaga K, Iwabuchi K, et al. Diffusion-weighted imaging of malignant breast tumors: the usefulness of apparent diffusion coefficient (ADC) value and ADC map for the detection of malignant breast tumors and evaluation of cancer extension. J Comput Assist Tomogr 2005; 29:644-9.
17. Yamashita Y, Namimoto T, Mitsuzaki K, et al. Mucin-producing tumor of the pancreas: diagnostic value of diffusion-weighted echo-planar MR imaging. Radiology 1998; 208:605-9.
18. Moteki T, Ishizaka H. Diffusion-weighted EPI of cystic ovarian lesions: evaluation of cystic contents using apparent diffusion coefficients. J Magn Reson Imaging 2000; 12:1014-9.
19. Kim T, Murakami T, Takahashi S, et al. Diffusion-weighted single-shot echoplanar MR imaging for liver disease. AJR Am J Roentgenol 1999; 173:393-8.
20. Paran Y, Bendel P, Margalit R, Degani H. Water diffusion in the different microenvironments of breast cancer. NMR Biomed 2004; 17:170-80.
21. Chang SC, Lai PH, Chen WL, et al. Diffusion-weighted MRI features of brain abscess and cystic or necrotic brain tumors: comparison with conventional MRI. Clin Imaging 2002; 26:227-36.
22. Tsushima Y, Takahashi-Taketomi A, Endo K. Magnetic resonance (MR) differential diagnosis of breast tumors using apparent diffusion coefficient (ADC) on 1.5-T. J Magn Reson Imaging 2009; 30:249-55.
23. Koh DM, Collins DJ. Diffusion-weighted MRI in the body: applications and challenges in oncology. AJR Am J Roentgenol 2007; 188:1622-35.
24. Woodhams R, Matsunaga K, Kan S, et al. ADC mapping of benign and malignant breast tumors. Magn Reson Med Sci 2005; 4:35-42.
25. Ruboseva E, Grell AS, De Maertelaer V, et al. Quantitative diffusion imaging in breast cancer: a clinical prospective study. J Magn Reson Imaging 2006; 24:319-24.
26. Kuroki Y, Nasu K, Kuroki S, et al. Diffusion-weighted imaging of breast cancer with the sensitivity encoding technique: analysis of apparent diffusion coefficient value. Magn Reson Med Sci 2004; 3:79-85.
27. Hatakenaka M, Soeda H, Yabuuchi H, et al. Apparent diffusion coefficients of breast tumors: clinical application. Magn Reson Med Sci 2008; 7:23-9.
28. Luo JD, Liu YY, Zhang XL, Shi LC. [Application of diffusion weighted resonance imaging to differential diagnosis of breast diseases]. Ai Zheng 2007; 26:168-71. Chinese.
29. Dorenbeck U, Butz B, Schlaier J, et al. Diffusion-weighted echo-plenar MRI of the brain with calculated ADCs: a useful tool in the differential diagnosis of tumor necrosis from abscess? J Neuroimaging 2003; 13:330-8.
30. Pereira FP, Martins G, Figueiredo E, et al. Assessment of breast lesions with diffusion-weighted MRI: comparing the use of different b values. AJR Am J Roentgenol 2009; 193:1030-5.
31. Belli P, Constantini M, Bufi E, et al. Diffusion-weighted imaging in breast lesion evaluation. Radiol Med 2010; 115:51-69.
32. Sinha S, Sinha U. Functional magnetic resonance of human breast tumors: diffusion and perfusion imaging. Ann N Y Acad Sci 2002; 980: 95-115.
33. Yabuuchi H, Matsuo Y, Kamitani T, et al. Non-mass-like enhancement on contrast-enhanced breast MR imaging: lesion characterization using combination of dynamic contrast-enhanced and diffusion-weighted MR images. Eur J Radiol 2010; 75:e126-32.
34. Warach S, Boska M, Welch KM. Pitfalls and potential of clinical diffusion-weighted MR imaging in acute stroke. Stroke 1997; 28:481-2.
35. Sugahara T, Korogi Y, Kochi M, Ikushima I, et al. Usefulness of diffusion-weighted MRI with echo-planar technique in the evaluation of cellularity in gliomas. J Magn Reson Imaging 1999; 9:53-60.